I&EC research
Industrial & Engineering Chemistry Research

Article

pubs.acs.org/IECR

Novel Magnetorheological Plastomer Filled with NdFeB Particles: Preparation, Characterization, and Magnetic−Mechanic Coupling Properties

Wenqiang Zhao, Haoming Pang, and Xinglong Gong*

CAS Key Laboratory of Mechanical Behavior and Design of Materials, Department of Modern Mechanics, University of Science and Technology of China, Hefei 230027, China

ABSTRACT: This work reported a novel magnetorheological plastomer doped with hard magnetic NdFeB particles (named as H-MRP). The dynamic properties of the H-MRP were systematically tested, and the mechanism of its unusual response to magnetic field was discussed. Unlike the MRP filled with soft magnetic particles (S-MRP), the storage modulus (G') of H-MRPs kept growing by 20% when the magnetic field decreased, while that of S-MRPs decreased with decreasing of the magnetic field immediately without an obvious change. Under the magnetic field ranging from 0 to 1 T, there was a peak value in the rising stage of G' at about 400 mT magnetic field, while that of S-MRPs changed monotonically. After an off−on progress of the magnetic field, the final G' of H-MRPs increased by over 10%. A possible mechanism was proposed to study the microstructure dependent mechanical properties. It was found that the complex viscoelastic behavior originated from the large hysteresis characteristics of the H-MRPs.

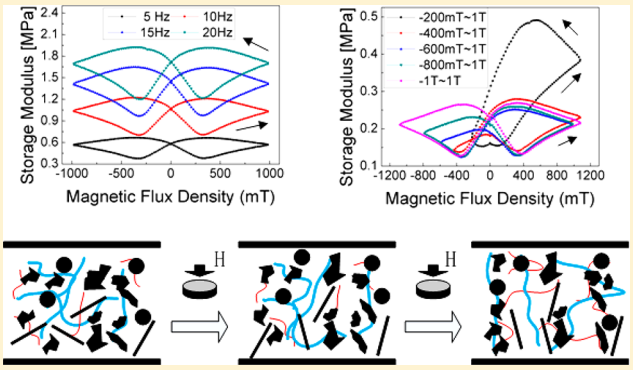

1. INTRODUCTION

Magnetorheological (MR) materials have attracted increasing attention since their unique rheological properties can be changed continuously, rapidly, and reversibly by applying a magnetic field. Due to the unique MR effects, the MR materials possess wide application in dampers,[1−5] shock absorbers,[6−8] isolators,[9−12] etc. The MR materials are usually prepared by dispersing magnetic particles into the carrier matrixes. According to the state of the matrix, MR materials can be classified into MR fluids, MR gels, MR foams, and MR elastomers.[13−15] The mostly studied MR material was MR fluids (MRFs), and the mechanism of an MRF[16−19] and its applications have been extensively studied. However, problems such as particle sediment, stability, and leakage in application devices existed. To solve these problems, polymer matrixes with high viscosities were employed to carry ferromagnetic particles and so-called MR gels (MRGs) and MR elastomers (MREs) were developed.[20−24] Recently, magnetorheological plastomers (MRPs) were developed by dispersing carbonyl iron powders in soft polymer matrixes because of their high MR effects and stability.[25−28] Owing to the unique magnetic field dependent microstructure and mechanical properties, MRPs possessed broad application prospects.[24,29]

Soft magnetic particles, such as carbonyl iron (CI) powders, were widely used in MR materials, because of their high saturation magnetization and low remanence. MRPs composed of soft CI particles were mostly reported. The iron powders in MRPs arrange to form particle chains while a magnetic field is applied. After removal of the magnetic field, the chainlike structures can be maintained for a period of time due to the viscidity of the matrix. Hard magnetic particles, with lower saturation magnetization, were mainly used in early studies.[30−33] But the presence of magnetic moments of hard magnetic particles has not been studied until now. In consideration of the soft matrix, the movable hard magnetic particles and their assembling structures determined that the unique mechanical characteristics of a magnetorheological plastomer filled with hard magnetic particles (H-MRP) would be different from those of the traditional magnetorheological plastomer filled with soft magnetic particles (S-MRP). Yu et al.[11] reported that the hard magnetic particle based MRE presented negative MR effects because of the large remanence. To this end, unusual MR behavior would be expected in H-MRP because the remanence forced the hard magnetic particles to form a special structure. Obviously, the structure-dependent mechanics must be very interesting and this phenomenon will be favorable for further understanding of the MR mechanism.

Here, a magnetorheological plastomer filled with hard magnetic particles was prepared. The dynamic properties of the H-MRP material were systematically tested and analyzed. Instead of a high magnetorheological effect, the H-MRP

Received: April 13, 2017
Revised: June 6, 2017
Accepted: July 21, 2017
Published: July 21, 2017

DOI: 10.1021/acs.iecr.7b01553
Ind. Eng. Chem. Res. 2017, 56, 8857−8863

exhibited more complex mechanical properties. In order to understand the phenomenon, a possible explanation is put forward to analyze its unique rheological behavior. All the experimental results indicated that the viscoelastic behavior resulted from the complex microstructure formed by the hard magnetic particles.

2. EXPERIMENTAL SECTION

2.1. Raw Materials. The materials used included toluene diisocyanate (TDI; 2,4-TDI at B 80%, 2,6-TDI at B 20%, Tokyo Chemical Industry Co. Ltd., Japan), polypropylene glycol (PPG-1000, Sinopec Group Co. Ltd., China), 1,4-butanediol (BDO; Sinopharm Chemical Reagent Co., Ltd., China), carbonyl iron powders (CIPs; type CN, BASF Aktiengesellschaft, Germany), and NdFeB particles (with a wide size distribution (1−100 μm), Guangzhou Nuode Transmission Parts Co. Ltd., China.)

2.2. Sample Preparation. There are three steps in the synthesis of the polymer matrix for the H-MRP. First, TDI and PPG with a molar ratio of 3:1 were added to a three-necked round-bottom flask with a stirrer agitating the reactants all the time; the temperature of the reaction system was 80 °C. After 2 h, BDO was added to the reactor. The temperature was reduced to 60 °C. After 30 min, ethyl alcohol (5 mL) was added to the flask. When the viscosity of the reactant increased obviously, the reaction was stopped.

The CIPs and NdFeB particles were added into the matrix by vigorously stirring for a long enough time until the matrix and particles were well mixed. After the composite was cooled, it was aged at room temperature for 72 h. Several samples with different fractions of magnetic particles were prepared, and the detailed compositions are listed in Table 1. In addition, matrix without any magnetic particles was also prepared.

Table 1. Compositions of Samples

	sample no.								
	1	2	3	4	5	6	7	8	9
PU (g)	10	10	10	10	10	10	10	10	10
NdFeB (g)	0	0	0	2.5	6.7	0	5	10	15
carbonyl iron (g)	0	2.5	6.7	0	0	15	10	5	0

2.3. Measurements of Dynamic Properties. The dynamic properties of the H-MRPs were measured with a rheometer (Physica MCR 301, Anton Paar Co., Austria). As shown in Figure 1, the test sample (diameter 20 mm and thickness 1 mm) was put between the rotating disk and the base. The direction of the magnetic field controlled by the electromagnet was parallel with the direction of thickness. The test was in an oscillating mode and all samples were tested at a strain amplitude of 0.1% and a temperature of 25 °C.

3. RESULTS AND DISCUSSION

Figure 2a,b presents SEM images of samples filled with NdFeB particles. Figure 2c,d presents SEM images of samples filled with a mixture of NdFeB and CIPs. It can be seen from Figure 2a,c that both NdFeB and CIPs were well dispersed in polyurethane (PU) matrix. The average size of NdFeB particles was 30 μm, which was 4 times larger than that of CIPs (6 μm). Therefore, the NdFeB particles were more difficult to move in the PU matrix than the carbonyl iron. When the magnetic field was applied on the H-MRP, the samples deformed and its

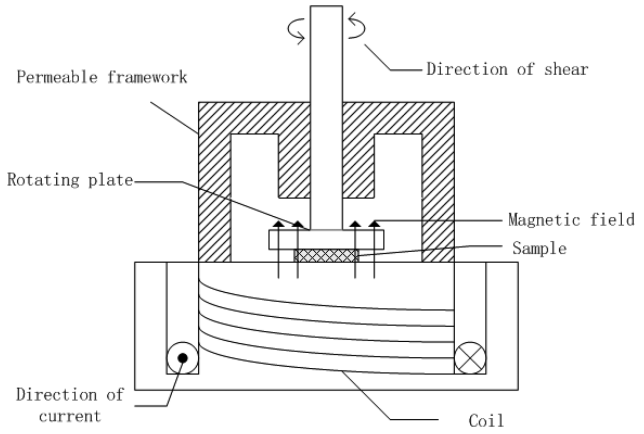

Figure 1. Schematic diagram of the Physica MCR 301 test system.

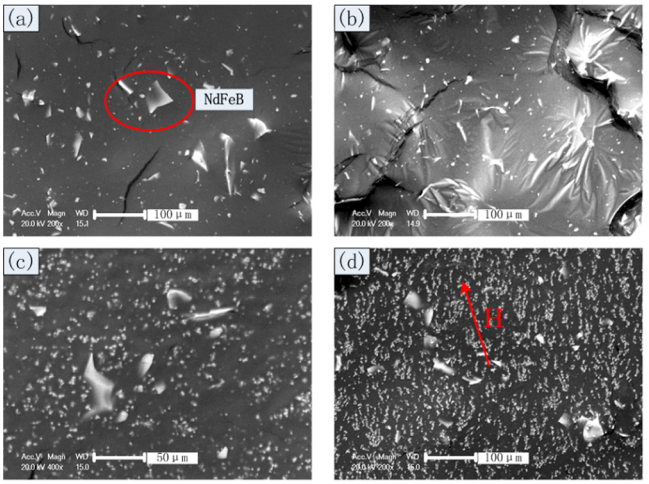

Figure 2. SEM images of MRP filled with NdFeB particles with a mass fraction of 60 wt % (a) not prestructured and (b) prestructured, and with NdFeB particles with mass fractions of 20 wt % CIPs and 40 wt % NdFeB (c) not prestructured and (d) prestructured.

surface became rough because the irregularly shaped NdFeB particles moved along the magnetic field with PU matrix around them. However, for Figure 2d, the surface was still smooth, which must be due to the lower mass rate of NdFeB particles. It can also be seen from Figure 2b,d that particles were arranged to form chain structures under the magnetic field. Figure 3 shows hysteresis loops of MRP with 60 wt % CIPs, 40 wt % CIPs and 20 wt % NdFeB particles, 20 wt % CIPs and 40 wt % NdFeB particles, and 60 wt % NdFeB

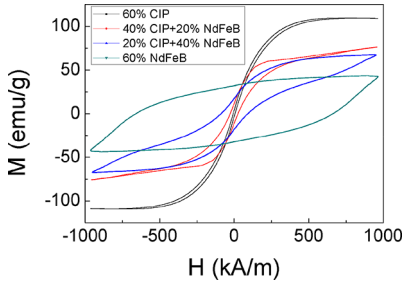

Figure 3. Hysteresis loops of MRP with 60 wt % CIPs, 40 wt % CIPs and 20 wt % NdFeB particles, 20 wt % CIPs and 40 wt % NdFeB particles, and 60 wt % NdFeB particles.

DOI: 10.1021/acs.iecr.7b01553
Ind. Eng. Chem. Res. 2017, 56, 8857−8863

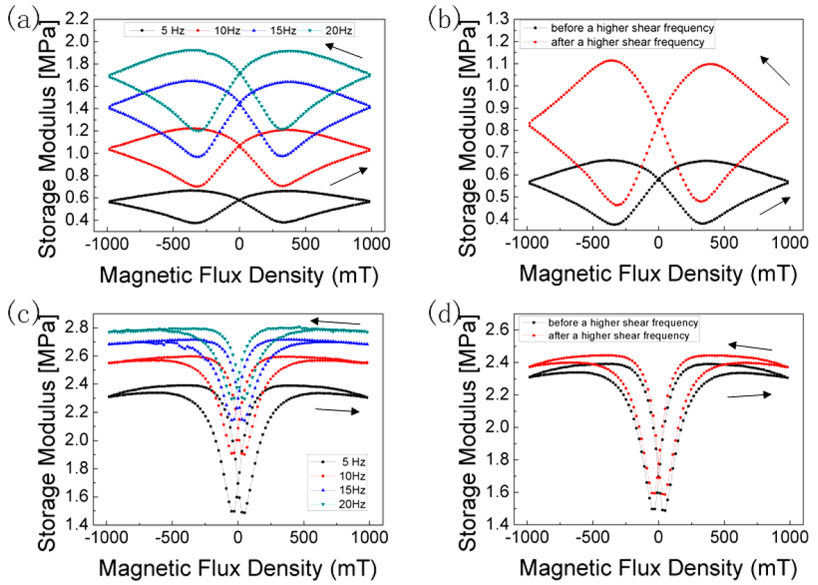

Figure 4. (a) G' of H-MRP with 60 wt % NdFeB particles to magnetic flux density with the magnetic field changing in the way of 0 T to 1 T to −1 T to 0 T. (b) G' of H-MRP to magnetic flux density before and after undergoing a higher shear frequency. (c) G' of S-MRP with 60 wt % CIPs to magnetic flux density with the magnetic field changing in the way of 0 T to 1 T to −1 T to 0 T. (d) G' of S-MRP to magnetic flux density before and after undergoing a higher shear frequency.

particles. The M_s of the NdFeB particles was 43.6 emu/g, which was much lower than that of the CIP. However, since pure NdFeB particles had a bigger remanence than CIPs (almost zero), the sample with a larger fraction of NdFeB particles presented a lower M_s and a larger remanence. M_s values of samples filled with the NdFeB/CIP mixture were between the two above, which showed the magnetic properties of MRPs changed with the NdFeB/CIP ratio.

Figure 4 shows the storage modulus of the sample under application of a magnetic field. Here, the magnetic field strength was started from 0 to 1 T and then decreased to 0 T. After that, the magnetic field strength further reduced to −1 T by changing the direction of the flowing current. At last, the magnetic field came back to 0 T again. During the test, the 0 T → 1 T → 0 T → −1 T → 0 T cycling magnetic field was applied on the 60 wt % H-MRP and S-MRP three times under a stable shear frequency. Then, the influences of the shear frequency on the storage moduli of the samples were investigated by varying the shear frequency from 5 to 20 Hz. Taking 5 Hz, for example, when the magnetic field increased from 0 to 1 T, G' reduced from 0.6 to 0.4 MPa at about 350 mT. Then it began to increase to about 0.6 MPa. Interestingly, the storage modulus underwent an increase−decrease process when the magnetic field began to decrease. While the magnetic field decreased from 1 T to 350 mT, G' kept increasing to 0.7 MPa. After that, G' began to reduce. It can be seen from Figure 3 that, in complete cycle scanning of the magnetic field, when the magnetic field was removed, the particles were not completely demagnetized. Thus, this sample would keep a high G' when the magnetic field was 0 T. Besides, when the magnetic field changed from 0 T to 350 mT, particles began to degauss, resulting in the decreasing of G'. The phenomenon that the G' did not reach the maximum when the magnetic field reached 1 T was in response to that the magnetic particles have not been saturated. Differently, the G' of 60 wt % S-MRP (Figure 4c) kept increasing with the increase of magnetic field.

The influence of the shear frequency on the mechanical properties of the H-MRP was investigated. With the increase of shear frequency, the G' increased. The difference between the maximum and the minimum of G' was larger, because the particles became harder to move under a higher shear frequency. Moreover, we made a comparison on the complete cycle magnetic field scanning of MRPs before and after undergoing a higher shear frequency (Figure 4b). It can be seen obviously that the scanning curve of MRPs changed after undergoing a high shear frequency. The minimum value increased from 0.37 to 0.5 MPa, and the maximum G' increased from 0.65 to 1.1 MPa. G' of MRPs with a magnetic field of 1 T increased from 0.55 to 0.83 MPa. Those changes resulted in a higher magnetorheological effect (from 176 to 220%). However, in Figure 4d, the scanning curve of S-MRPs stayed almost the same. The minimum value increased from 1.5 to 1.6 MPa, and the maximum increased from 2.38 to 2.43 MPa. G' of S-MRPs with a magnetic field of 1 T increased from 2.3 to 2.38 MPa. The magnetorheological effects were almost the same (from 159 to 152%). This difference originated from the remanence of the hard magnetic particles. The chaotic particles were aligned along the direction of the magnetic field under the magnetic field and oscillatory shear, making the subsequent magnetic response more pronounced.

The magnetic behavior of MRPs mainly depends on the magnetic properties of the filled particles. Due to the small remanence of CIP, G' values of S-MRPs under the magnetic field in the rising stage and descent stage are almost the same. However, G' values of H-MRPs showed different properties. In this work, samples were tested under an incomplete cycle of magnetic field. The maximum of the positive magnetic field was fixed at 1 T. The maximum of the negative magnetic field changed from 200 mT to 1 T, in steps of 200 mT. As shown in Figure 5, when the maximum of the negative magnetic field was larger than 400 mT, the curves had the same trend as with the magnetic field change from 0 to 1 T. All of those curves reached the lowest point at about 400 mT. However, the curve with a maximum of 200 mT exhibited differently. The G' was almost twice the others when the magnetic field reached 1 T. Besides, the shapes of the curves were different. The highest and lowest

DOI: 10.1021/acs.iecr.7b01553
Ind. Eng. Chem. Res. 2017, 56, 8857−8863

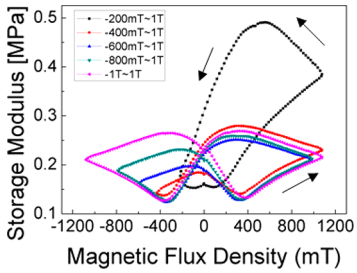

Figure 5. Asymmetric magnetic field scans of MRP with 60 wt % NdFeB particles. The maximum of the positive magnetic field was fixed to 1 T. The maximum of the negative magnetic field ranged from 200 mT to 1 T.

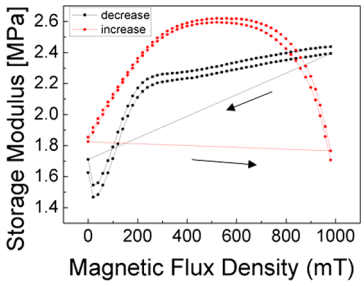

Figure 7. Response of G' of H-MRPs with 60 wt % NdFeB particles to a sudden decrease (case 1)/increase (case 2) of the magnetic field with a step of 1 T.

G' values of the samples were at different points of the magnetic field. It can be seen that the difference between such curves mainly depended on the peak value of the maximum negative magnetic field. If the maximum negative magnetic field was higher than 400 mT, NdFeB was degaussed and the microstructure of the sample became disordered; the lowest G' was obtained. Then, samples began to undergo a new cycle with the same start, so the positive axes of those curves were similar. If the maximum of the negative magnetic field was lower than 400 mT, NdFeB was not fully degaussed, and chainlike structures were still maintained. The magnetic state and structure of the sample changed, so the sample began to undergo a new cycle with a more ordered structure, resulting in an increase in G'.

Figure 6 shows responses of G' of H-MRPs under the magnetic field range from 0 mT to 1 T. In Figure 6a, H-MRPs were well prestructured and then tested under a cycle of magnetic field. The rising stage of the curve of S-MRPs was similar to the descent stage. However, H-MRPs were not the same. G' of H-MRPs rose to 0.85 MPa rapidly from 0.6 MPa when the magnetic field began to rise. At 300 mT, it dropped to a small value. At the magnetic field of 350 mT, it began to rise again. The peak G' was the result of the destruction of the structure formed by the remanent magnetization. In Figure 6b, a cyclic magnetic field was applied to the H-MRPs during the tests. It can be seen that the maximum of G' increased from 0.45 to 0.8 MPa with increasing cycle number, proving that cyclic magnetization strengthened the H-MRPs.

A sudden change of magnetic field was applied in order to observe the mechanical behavior of H-MRPs (Figure 7). We found that G' of H-MRPs changed differently when the magnetic field increased or decreased. In case 1, the magnetic field increased from 0 to 1 T, and then dropped to 0 T suddenly. G' of the sample decreased rapidly from 2.3 to 1.7 MPa immediately. Relatively, in case 2, the magnetic field decreased from 1 to 0 T, and then jumped to 1 T. G' of the sample did not increase immediately as was thought, but it stayed at 1.8 MPa. The change of G' in case 1 was similar to that of 0 to 1 T magnetic field scanning, but the change of G' in case 2 was different. G' increased with the decrease of magnetic field, and stayed at 2.6 MPa during the magnetic field range from 700 to 400 mT. Then it began to decrease. The instantaneous drop of the magnetic field would cause the H-MRP to decrease quickly, while the momentary jump in the magnetic field would have no instantaneous effect on the H-MRP. This showed that the sample under the action of the magnetic field underwent an elastic deformation process. This process would soon be able to recover after removal of the magnetic field.

The response of G' of MRPs under constant 1 T magnetic field was recorded in Figure 8. Figure 8a shows that G' of S-MRP increased to 2.4 MPa in a short time. Then it decreased a small amount to 2.2 MPa. As a comparison, G' of H-MRPs first decreased and then increased. Taking H-MRP with a 60 wt % NdFeB for an example, G' decreased to 0.6 MPa, and then kept increasing. The increase did not stop within 300 s. In Figure 8b, the sample underwent several cycles with the magnetic field jumping between 0 and 1 T. It can be seen that, after the removal of the magnetic field, G' of the H-MRP decreased rapidly and then increased. In every 1 T stage of the magnetic field, G' of the H-MRP tends to reach a limit value. However, the limit value was increasing as the cycle number increased. G' values of the H-MRP in the 1 T stage and the 0 T stage of the magnetic field are shown in Figure 8c,d. Both kept increasing, indicating that a 0 T stage of the magnetic field was useful to increasing G' of H-MRPs. Obviously, NdFeB played a key role in this phenomenon. After that, a change of the direction of the magnetic field was applied to H-MRP. Figure 8e shows a

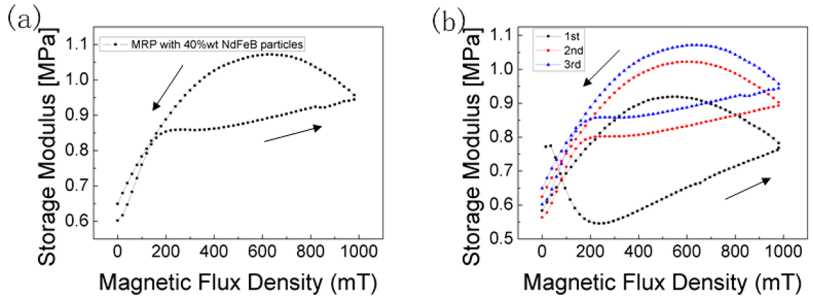

Figure 6. (a) Single and (b) multiple 0 T to 1 T to 0 T magnetic field scanning of MRP with 40 wt % NdFeB particles. The magnetic field changed from 0 to 1 T, and then changed back to 0 T slowly.

DOI: 10.1021/acs.iecr.7b01553
Ind. Eng. Chem. Res. 2017, 56, 8857−8863

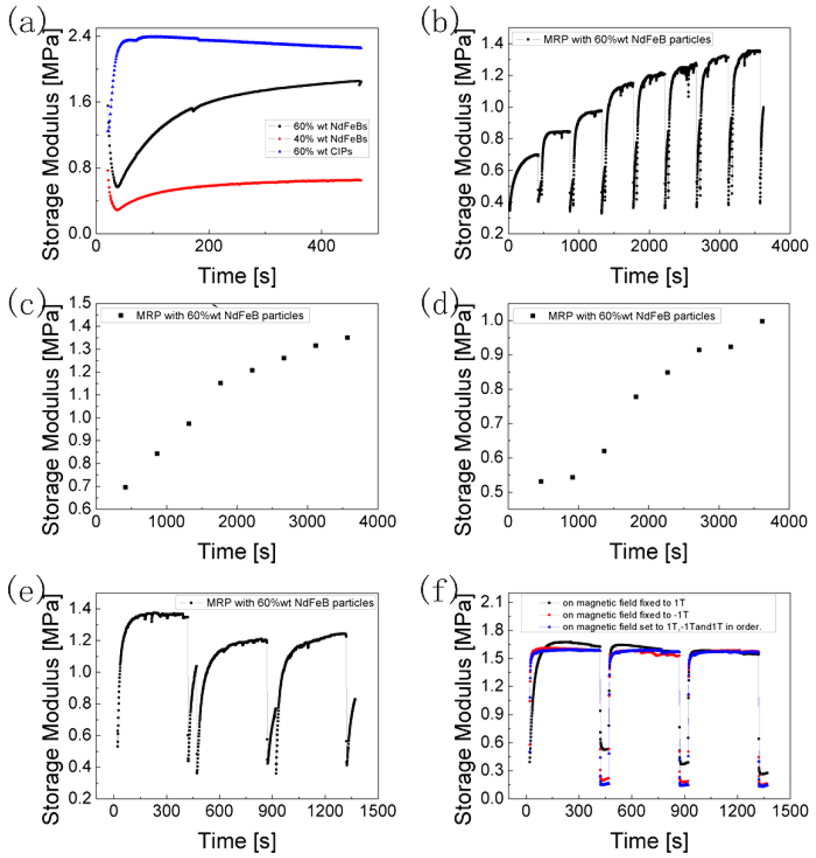

Figure 8. Constant magnetic field scanning of MRPs. (a) G' of MRP with 60 wt % NdFeB, 40 wt % NdFeB, and 60 wt % CIPs to a constant value of magnetic field fixed to 1 T. (b) On−off process of magnetic field with the on field fixed to 1 T. (c) Final G' of every on process of (b). (d) Final G' of every off process of (b). (e) Three cycles of on−off process with the magnetic field the second time fixed to −1 T. (f) G' of MRP with 60 wt % CIPs to the magnetic field in three types of on−off process (fixed to 1 and −1 T, and changed from 1 to −1 T only in the second cycle).

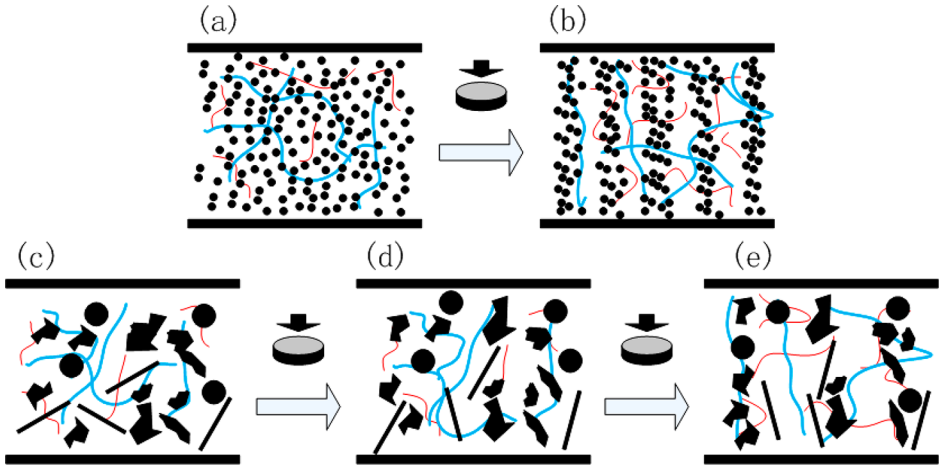

Figure 9. Schematic diagram of the change of microstructure process of MRPs under an external magnetic field: (a) S-MRP without a magnetic field. (b) S-MRPs with a magnetic field. (c) H-MRPs without a magnetic field. (d) Rotation of the particles in H-MRPs with magnetic field. (e) Rearrangement of the particles in H-MRPs with the magnetic field. Solid arrows indicate the direction of the magnetic field. Blue thick curves indicate the hard segments in PU, and the red thin ones indicate the soft segments.

progress of 1 T → 0 T → −1 T → 0 T → 1 T of the magnetic field. It can be seen that when the direction of the magnetic field was changed, G' of H-MRPs dropped from 1.35 to 1.2 MPa, which was caused by the rearrangement of the structure. Figure 8f shows G' of S-MRP filled with CIPs with a mass fraction of 60% in such cases, on a magnetic field fixed to 1 and −1 T, and changed from 1 to −1 T only in the second cycle. It is obvious that S-MRPs could not change with those cases, indicating that differences between H-MRPs and S-MRPs were mainly caused by hysteresis characteristics of NdFeB.

The differences between properties of S-MRPs and H-MRPs mainly resulted from the hysteresis characteristics and shapes of the particles. The mechanism of magnetorheological behavior of S-MRPs can be explained with Figure 9a,b.[25] For the

DOI: 10.1021/acs.iecr.7b01553
Ind. Eng. Chem. Res. 2017, 56, 8857−8863

situation without a magnetic field, the CIPs were distributed homogeneously in the matrix (as shown in Figure 9a). Increasing the magnetic field, the CIPs would eventually form chains aligned with the direction of the magnetic field (Figure 2). These particle chains ran through the whole material (as shown in Figure 9b). Due to the small coercivity, the CIPs would almost not rotate in the presence of the magnetic field. However, hard magnetic particles, such as NdFeB, would not form chains with the magnetic field immediately. As shown in Figure 2, the NdFeB particles were 10 times larger than CIPs; thus they could not move freely. It can be seen in Figure 2b that the surface of the sample became rough when it was put under a magnetic field. What is more, the shapes of NdFeB were irregular. The magnetic moments forced the hard magnetic particles to be rotated under the applied magnetic field. Therefore, the time of structural change needs to be considered for the H-MRPs (Figure 9c–e). For the situation without a magnetic field, particles distributed almost homogeneously in the matrix (as shown in Figure 9c). With increase of the magnetic field, particles started to undergo two processes. First, the NdFeB formed chainlike structures; thus the G' increased by this kind of process. For the second, the NdFeB particles rotated since the magnetic moment tended to transform along the magnetic field, which showed a small effect on the modulus. For NdFeB particles, the second process was much quicker than the first one; therefore the G' of H-MRP would not change as fast as that of S-MRP (Figure 4). As shown in Figure 4a, the G' increased when H decreased. This phenomenon can be easily explained by the second process. In Figure 5, differences between the first curve and the other four are mainly caused by the second process. When the negative magnetic field was larger than H_0, the particles were magnetized in the reverse direction and began to rearrange. The second process was a viscoelastic process, and with decreasing of the magnetic field, the G' decreased quicker than that of the increase (Figure 7). The rotation of the particles caused by the magnetic field made H-MRPs unstable, so G' kept changing when the magnetic field was removed (Figure 8b).

4. CONCLUSION

This work reported a novel NdFeB filled magnetorheological plastomer. The dynamic properties of the H-MRP materials were systematically tested and analyzed. Unlike traditional S-MRPs, the mechanical behavior of H-MRPs was more complex. G' of H-MRPs kept increasing when the magnetic field decreased, while that of S-MRPs decreased with the magnetic field immediately. In the incomplete magnetic field scan cycle, G' of H-MRPs increased slightly. After going through a peak value, it kept increasing again, while that of S-MRPs changed monotonically through both complete and incomplete cycle scans. Besides, the final G' of H-MRPs placed under a constant magnetic field remained stable but increased after an on–off progress of the magnetic field. However, it went back to the initial value when an opposite magnetic field was applied. All the experimental results indicated that viscoelastic behavior resulted from a more complex microstructure in MR materials, which should receive more attention to understand the MR mechanism.

AUTHOR INFORMATION

Corresponding Author

*E-mail: gongxl@ustc.edu.cn.

ORCID

Xinglong Gong: 0000-0001-6997-9526

Notes

The authors declare no competing financial interest.

ACKNOWLEDGMENTS

Financial support from the National Natural Science Foundation of China (Grant 11572309) and the Strategic Priority Research Program of the Chinese Academy of Sciences (Grant XDB22040502) is gratefully acknowledged. This study was also supported by the Collaborative Innovation Center of Suzhou Nano Science and Technology.

REFERENCES

(1) Sohn, J. W.; Oh, J. S.; Choi, S. B. Design and novel type of a magnetorheological damper featuring piston bypass hole. *Smart Mater. Struct.* **2015**, *24*, 035013.

(2) Xing, Z. W.; Yu, M.; Sun, S. S.; Fu, J.; Li, W. H. A hybrid magnetorheological elastomer-fluid (MRE-F) isolation mount: development and experimental validation. *Smart Mater. Struct.* **2016**, *25*, 015026.

(3) Li, W. H.; Yao, G. Z.; Chen, G.; Yeo, S. H.; Yap, F. F. Testing and steady state modeling of a linear MR damper under sinusoidal loading. *Smart Mater. Struct.* **2000**, *9*, 95–102.

(4) Raja, P.; Wang, X. J.; Gordaninejad, F. A high-force controllable MR fluid damper-liquid spring suspension system. *Smart Mater. Struct.* **2014**, *23*, 015021.

(5) Gong, X. L.; Fan, Y. C.; Xuan, S. H.; Xu, Y. G.; Peng, C. Control of the Damping Properties of Magnetorheological Elastomers by Using Polycaprolactone as a Temperature-Controlling Component. *Ind. Eng. Chem. Res.* **2012**, *51*, 6395–6403.

(6) Nguyen, Q. H.; Choi, S. B. Optimal design of MR shock absorber and application to vehicle suspension. *Smart Mater. Struct.* **2009**, *18*, 035012.

(7) Sun, S. S.; Yang, J.; Li, W. H.; Deng, H. X.; Du, H. P.; Alici, G.; Yan, T. H. An innovative MRE absorber with double natural frequencies for wide frequency bandwidth vibration absorption. *Smart Mater. Struct.* **2016**, *25*, 055035.

(8) Sun, S. S.; Yang, J.; Li, W. H.; Deng, H. X.; Du, H. P.; Alici, G. Development of an MRE adaptive tuned vibration absorber with self-sensing capability. *Smart Mater. Struct.* **2015**, *24*, 095012.

(9) Brigley, M.; Choi, Y. T.; Wereley, N. M.; Choi, S. B. Magnetorheological isolators using multiple fluid modes. *J. Intell. Mater. Syst. Struct.* **2007**, *18*, 1143–1148.

(10) Przybylski, M.; Sun, S. S.; Li, W. H. Development and characterization of a multi-layer magnetorheological elastomer isolator based on a Halbach array. *Smart Mater. Struct.* **2016**, *25*, 105015.

(11) Yu, M.; Zhao, L. J.; Fu, J.; Zhu, M. Thermal effects on the laminated magnetorheological elastomer isolator. *Smart Mater. Struct.* **2016**, *25*, 115039.

(12) Behrooz, M.; Wang, X. J.; Gordaninejad, F. Modeling of a new semi-active/passive magnetorheological elastomer isolator. *Smart Mater. Struct.* **2014**, *23*, 045013.

(13) Carlson, J. D.; Jolly, M. R. MR fluid, foam and elastomer devices. *Mechatronics* **2000**, *10*, 555–569.

(14) Fuchs, A.; Xin, M.; Gordaninejad, F.; Wang, X. J.; Hitchcock, G. H.; Gecol, H.; Evrensel, C.; Korol, G. Development and characterization of hydrocarbon polyol polyurethane and silicone magnetorheological polymeric gels. *J. Appl. Polym. Sci.* **2004**, *92*, 1176–1182.

(15) Kaleta, J.; Lewandowski, D. Inelastic properties of magnetorheological composites: I. Fabrication, experimental tests, cyclic shear properties. *Smart Mater. Struct.* **2007**, *16*, 1948–1953.

(16) Ginder, J. M.; Davis, L. C.; Elie, L. D. Rheology of magnetorheological fluids: Models and measurements. *Int. J. Mod. Phys. B* **1996**, *10*, 3293–3303.

(17) Yin, H. M.; Sun, L. Z. Magnetoelasticity of chain-structured ferromagnetic composites. *Appl. Phys. Lett.* **2005**, *86*, 261901.

DOI: 10.1021/acs.iecr.7b01553
Ind. Eng. Chem. Res. 2017, 56, 8857–8863

(18) Zubieta, M.; Eceolaza, S.; Elejabarrieta, M. J.; Bou-Ali, M. M. Magnetorheological fluids: characterization and modeling of magnetization. *Smart Mater. Struct.* **2009**, *18*, 095019.
(19) Kwon, S. H.; Hong, C. H.; Do, P. X.; Choi, S. B.; Choi, H. J. Magnetorheology of a Carbonyliron Microsphere Suspension with a Halloysite Additive and Its Damping Force Characteristics. *Ind. Eng. Chem. Res.* **2015**, *54*, 4655−4663.
(20) Boczkowska, A.; Awietjan, S. F.; Wroblewski, R. Microstructure-property relationships of urethane magnetorheological elastomers. *Smart Mater. Struct.* **2007**, *16*, 1924−1930.
(21) Woods, B. K. S.; Wereley, N.; Hoffmaster, R.; Nersessian, N. Manufacture of bulk magnetorheological elastomers using vacuum assisted resin transfer molding. *Int. J. Mod. Phys. B* **2007**, *21*, 5010−5017.
(22) Wang, Y.; Gong, X. L.; Yang, J.; Xuan, S. H. Improving the Dynamic Properties of MRE under Cyclic Loading by Incorporating Silicon Carbide Nanoparticles. *Ind. Eng. Chem. Res.* **2014**, *53*, 3065−3072.
(23) Fan, Y. C.; Gong, X. L.; Xuan, S. H.; Qin, L. J.; Li, X. F. Effect of Cross-Link Density of the Matrix on the Damping Properties of Magnetorheological Elastomers. *Ind. Eng. Chem. Res.* **2013**, *52*, 771−778.
(24) Ju, B. X.; Yu, M.; Fu, J.; Zheng, X.; Liu, S. Z. Magnetic Field-Dependent Normal Force of Magnetorheological Gel. *Ind. Eng. Chem. Res.* **2013**, *52*, 11583−11589.
(25) Xu, Y. G.; Gong, X. L.; Xuan, S. H.; Zhang, W.; Fan, Y. C. A high-performance magnetorheological material: preparation, characterization and magnetic-mechanic coupling properties. *Soft Matter* **2011**, *7*, 5246−5254.
(26) Xu, Y. G.; Gong, X. L.; Xuan, S. H.; Li, X. F.; Qin, L. J.; Jiang, W. Q. Creep and recovery behaviors of magnetorheological plastomer and its magnetic-dependent properties. *Soft Matter* **2012**, *8*, 8483−8492.
(27) Xu, Y. G.; Gong, X. L.; Liu, T. X.; Xuan, S. H. Magneto-induced microstructure characterization of magnetorheological plastomers using impedance spectroscopy. *Soft Matter* **2013**, *9*, 7701−7709.
(28) Liu, T. X.; Gong, X. L.; Xu, Y. G.; Xuan, S. H.; Jiang, W. Q. Simulation of magneto-induced rearrangeable microstructures of magnetorheological plastomers. *Soft Matter* **2013**, *9*, 10069−10080.
(29) Pang, H. M.; Xuan, S. H.; Liu, T. X.; Gong, X. L. Magnetic field dependent electro-conductivity of the graphite doped magnetorheological plastomers. *Soft Matter* **2015**, *11*, 6893−6902.
(30) Koo, J. H.; Dawson, A.; Jung, H. J. Characterization of actuation properties of magnetorheological elastomers with embedded hard magnetic particles. *J. Intell. Mater. Syst. Struct.* **2012**, *23*, 1049−1054.
(31) Siegfried, P.; Koo, J. H.; Pechan, M. Torque characterization of functional magnetic polymers using torque magnetometry. *Polym. Test.* **2014**, *37*, 6−11.
(32) Stepanov, G. V.; Chertovich, A. V.; Kramarenko, E. Y. Magnetorheological and deformation properties of magnetically controlled elastomers with hard magnetic filler. *J. Magn. Magn. Mater.* **2012**, *324*, 3448−3451.
(33) Kramarenko, E. Y.; Chertovich, A. V.; Stepanov, G. V.; Semisalova, A. S.; Makarova, L. A.; Perov, N. S.; Khokhlov, A. R. Magnetic and viscoelastic response of elastomers with hard magnetic filler. *Smart Mater. Struct.* **2015**, *24*, 035002.

DOI: 10.1021/acs.iecr.7b01553
Ind. Eng. Chem. Res. 2017, 56, 8857−8863